REVISTA INTERDISCIPLINAR DE PESQUISA EM ENGENHARIA

CILAMCE 2016
XXXVII IBERIAN LATIN AMERICAN CONGRESS ON COMPUTATIONAL METHODS IN ENGINEERING
BRASÍLIA - DF - BRAZIL

NONLINEAR VIBRATIONS OF FLUID-FILLED VISCOELASTIC CYLINDRICAL SHELLS

Zenon J. G. N. del Prado

zenon@ufg.br

Universidade Federal de Goias, Escola de Engenharia Civil, Avenida Universitária, 1488, Setor Leste Universitário, 74605-200, Goiânia, GO, Brazil

Marco Amabili

marco.amabili@mcgill.ca

Department of Mechanical Engineering, McGill University, 817 Sherbrooke Street West, Montreal, Canada H3A 0C3

Paulo B. Gonçalves

paulo@puc-rio.br

Catholic University of Rio de Janeiro, Department of Civil Engineering, Rua Marquês de São Vicente, 225, Gávea, 22453-900, Rio de Janeiro, RJ, Brazil

Frederico M. Alves da Silva

silvafma@ufg.br

Universidade Federal de Goias, Escola de Engenharia Civil, Avenida Universitária, 1488, Setor Leste Universitário, 74605-200, Goiânia, GO, Brazil

Abstract. *In this work the non-linear vibrations of a simply supported viscoelastic fluid-filled circular cylindrical shells subjected to lateral harmonic load is studied. Donnell's non-linear shallow shell theory is used to model the shell, assumed to be made of a Kelvin-Voigt material type, and a modal solution with six degrees of freedom is used to describe the lateral displacements. The Galerkin method is applied to derive a set of coupled non-linear ordinary differential equations of motion. The influence of shell geometry, flow velocity and dissipation parameter are studied and special attention is given to resonance curves. Obtained results show that the viscoelastic dissipation parameter, flow velocity and geometry have significant influence on the nonlinear behavior of the shells as displayed in instability loads and resonance curves.*

Keywords: *Cylindrical shells, Viscoelastic material, Fluid-structure interaction, Nonlinear vibrations*

1 INTRODUCTION

Viscoelastic materials are frequently used in sandwich structures such as beams, plates and shells where damping is desired for a wide range of frequencies. However, in spite of a large number of studies on cylindrical shell dynamics, just a small number of these works is related to the analysis of viscoelastic shells.

Cheng and Zhang (2001) and Cederbaum and Touati (2002) studied the nonlinear dynamic behavior of viscoelastic cylindrical shells subjected to axial loads using the Von Kármán-Donnell non-linear shell theory. Seeking to observe the effect of lateral pressures, Antman and Lacarbonara (2009) studied the radial motions of compressible non-linearly viscoelastic cylindrical and spherical shells under time-dependent pressures. Also, Shina et al (2009) applied the finite element method to study the thermal post-buckled characteristics of cylindrical composite shells with viscoelastic layers, considering transversal shear deformation and variable in-plane displacements through the thickness of the shell.

In a series of papers Eshmatov (2007a, 2007b, 2007c, 2007d, 2008, 2009) studied the vibrations and dynamic stability of viscoelastic cylindrical shells and cylindrical panels with and without concentrated masses using the Kirchhoff-Love hypothesis and Timoshenko theories by taking into account shear deformation and rotary inertia. The influence of viscoelastic material properties and the critical loads were evaluated.

Lacarbonara and Antman (2012) analyzed the radial motions of cylindrical and spherical shells under pulsating pressures considering non-linear viscoelasticity. In this study a rich non-linear dynamic behavior was observed with softening and hardening curves on the primary region of resonance depending on the constitutive functions and external loads.

Mohammadi and Sedaghati (2012) analyzed the vibration of sandwich cylindrical shells with thin or thick core layer based on a new higher-order expansion of transverse and in-plane displacement fields in the thickness direction of the core layer. Recently, Alijani and Amabili (2013) wrote a detailed literature review of current studies on non-linear vibrations of shells where the reduced number of studies dedicated to the analysis of viscoelastic cylindrical shells can be confirmed.

In the present paper, the influence of load and material properties on the non-linear vibrations and dynamic instability of a simply supported viscoelastic circular fluid-filled cylindrical shells subjected to lateral harmonic load is studied. Donnell's non-linear shallow shell theory is used to model the shell, which is assumed to be made of a Kelvin-Voigt material type, and a modal solution with six and eight degrees of freedom which takes into account the essential modal couplings and interactions is used to describe the lateral displacements of the shell. The Galerkin method is applied to derive a set of coupled non-linear ordinary differential equations of motion that are, in turn, solved by the Runge-Kutta method. The obtained results show that the viscoelastic dissipation parameter has a very significant influence on the instability loads and resonance of the viscoelastic shells and, depending on the applied load and dissipation parameter.

2 MATHEMATICAL FORMULATION

Consider a perfect thin-walled fluid-filled simply supported circular cylindrical shell of radius R, length L and thickness h. The axial, circumferential and radial coordinates are denoted by x, $y = R\theta$ and z, respectively, and the corresponding displacements of the shell middle surface are denoted by u, v and w, as shown in Figure 1. The shell is assumed to be made of a Kelvin-Voigt viscoelastic material with initial Young's modulus E, Poisson ratio ν, and density ρ.

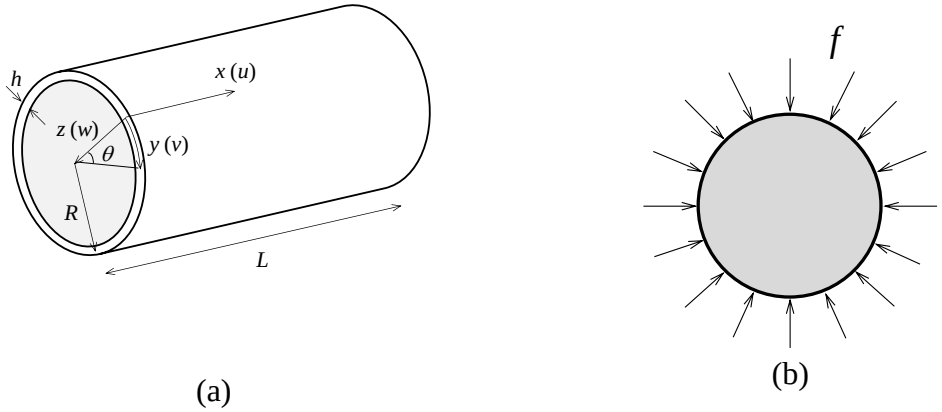

Figure 1. Shell characteristics. (a) Shell geometry; (b) Harmonic lateral pressure *f*.

The shell is subjected to the following harmonic lateral pressure:

$$f = F_L h^2 \rho \omega_o^2 \sin\left(\frac{m\pi x}{L}\right)\cos(n\theta)\cos(\omega_L t) \tag{1}$$

where F_L is the nondimensional coefficient of the amplitude of the load, ω_0 is the natural frequency of the shell, m ,the number of axial half-waves, n , the circumferential wave number, ω_L , the frequency of the load and t the time.

Based on Donnell shallow-shell theory, the middle surface kinematic relations are given, in terms of the three displacement components, by:

$$\varepsilon_{x,0} = u_{,x} + \frac{1}{2}w_{,x}^2, \qquad \varepsilon_{\theta,0} = \frac{v_{,\theta}}{R} - \frac{w}{R} + \frac{1}{2}\frac{w_{,\theta}^2}{R^2}, \qquad \gamma_{x\theta,0} = \frac{u_{,\theta}}{R} + v_{,x} + w_{,x}\frac{w_{,\theta}}{R},$$
$$\chi_{xx} = -w_{,xx}, \qquad \chi_{\theta\theta} = -\frac{w_{,\theta\theta}}{R^2}, \qquad \chi_{x\theta} = -\frac{w_{,x\theta}}{R}, \tag{2}$$

where $\varepsilon_{x,0}$ and $\varepsilon_{\theta,0}$ are the strains in the axial and circumferential directions, $\gamma_{x\theta,0}$ is the shearing strain component at a point on the shell middle surface, χ_{xx} and $\chi_{\theta\theta}$ are the curvature changes and $\chi_{x\theta}$ is the twist.

The strain components ε_{xx}, $\varepsilon_{\theta\theta}$ and $\gamma_{x\theta}$ at an arbitrary point of the shell are related to the middle surface strains $\varepsilon_{x,0}$, $\varepsilon_{\theta,0}$ and $\gamma_{x\theta,0}$ and to the changes in the curvature by the following relations:

$$\varepsilon_{xx} = \varepsilon_{x,0} + z\chi_{xx}, \qquad \varepsilon_{\theta\theta} = \varepsilon_{\theta,0} + z\chi_{\theta\theta}, \qquad \gamma_{x\theta} = \gamma_{x\theta,0} + z\chi_{x\theta}. \tag{3}$$

In this analysis, the viscoelastic behavior of the material is modeled in the base of the Kelvin-Voigt viscoelastic theory. This viscoelastic model can be represented by a viscous damper element and an elastic spring element connected in parallel as illustrated in Fig. 2.

Considering the plane stress problem and the Kelvin-Voigt constitutive model of a viscoelastic material, the stress-strain relations can be written as (Esmailzade, 1999):

$$\sigma_{xx} = \frac{E}{1-\nu^2}\left[\varepsilon_{xx} + \nu\,\varepsilon_{\theta\theta} + \eta\frac{d}{dt}\left(\varepsilon_{xx} + \nu\,\varepsilon_{\theta\theta}\right)\right] \tag{4}$$

$$\sigma_{\theta\theta} = \frac{E}{1-\nu^2}\left[\varepsilon_{\theta\theta} + \nu\,\varepsilon_{xx} + \eta\frac{d}{dt}\left(\varepsilon_{\theta\theta} + \nu\,\varepsilon_{xx}\right)\right] \tag{5}$$

$$\sigma_{x\theta} = \frac{E}{2(1+\nu)}\left[\gamma_{x\theta} + \eta\frac{d}{dt}\left(\gamma_{x\theta}\right)\right] \tag{6}$$

where E is the Young's modulus, ν is the Poisson coefficient, t is the time and η is the coefficient of the viscoelastic dissipation parameter, also named retardation time, and it is measured in seconds.

Using the stress function F, the forces in the axial, circumferential and tangential directions are

$$N_x = \frac{1}{R^2}\frac{\partial^2 F}{\partial\,\theta^2}, \qquad N_\theta = \frac{\partial^2 F}{\partial\,x^2}, \qquad N_{x\theta} = -\frac{1}{R}\frac{\partial^2 F}{\partial x\,\partial\theta}. \tag{7}$$

The non-linear equation of motion, based on the Donnell shallow shell theory, in terms of a stress function F, the lateral displacement w is given by:

$$\begin{aligned}&\frac{Eh^3}{12(1-\nu^2)}\left[\frac{\partial^4 w}{\partial x^4} + \frac{2}{R^2}\frac{\partial^4 w}{\partial x^2\,\partial\theta^2} + \frac{1}{R^4}\frac{\partial^4 w}{\partial\theta^4}\right] + \frac{Eh^3}{12(1-\nu^2)}\eta\frac{\partial}{\partial t}\left[\frac{\partial^4 w}{\partial x^4} + \frac{2}{R^2}\frac{\partial^4 w}{\partial x^2\,\partial\theta^2} + \frac{1}{R^4}\frac{\partial^4 w}{\partial\theta^4}\right]\\ &+ c\,h\frac{\partial w}{\partial t} + \rho\,h\frac{\partial^2 w}{\partial t^2} = f + P_h + \frac{1}{R^2}\frac{\partial^2 F}{\partial\,\theta^2}\frac{\partial^2 w}{\partial\,x^2} - 2\frac{1}{R^2}\frac{\partial^2 F}{\partial x\,\partial\theta}\frac{\partial^2 w}{\partial x\,\partial\theta} + \frac{\partial^2 F}{\partial\,x^2}\left(\frac{\partial^2 w}{R^2\,\partial\theta^2} + \frac{1}{R}\right)\end{aligned} \tag{8}$$

where $c = 2\zeta\rho\omega_o$ (kg/m^3 s) is the viscous damping coefficient, ζ is the viscous damping ratio of the shell, P_h is the perturbation pressure due to steady internal fluid and f is the radial pressure applied to the surface of the shell due to external force. In equation (8) a global viscous damping has been introduced in addition to the viscoelasticity of the shell material.

The compatibility equation is given by

$$\frac{\partial^4 F}{\partial x^4}+\frac{2}{R^2}\frac{\partial^4 F}{\partial x^2\partial\theta^2}+\frac{1}{R^4}\frac{\partial^4 F}{\partial\theta^4}=E\,h\left[-\frac{1}{R}\frac{\partial^2 w}{\partial x^2}+\frac{1}{R^2}\left(\frac{\partial^2 w}{\partial x\partial\theta}\right)^2-\frac{1}{R^2}\frac{\partial^2 w}{\partial x^2}\frac{\partial^2 w}{\partial\theta^2}+\right.$$
$$\left.\eta\left(-\frac{1}{R^2}\frac{\partial^3 w}{\partial x^2\partial t}\frac{\partial^2 w}{\partial\theta^2}-\frac{1}{R^2}\frac{\partial^2 w}{\partial x^2}\frac{\partial^3 w}{\partial\theta^2\partial t}-\frac{1}{R}\frac{\partial^3 w}{\partial x^2\partial t}+\frac{2}{R^2}\frac{\partial^3 w}{\partial x\partial\theta\partial t}\frac{\partial^2 w}{\partial x\partial\theta}\right)\right]. \tag{9}$$

The simply supported out-of-plane (Eq. 10) and the in-plane (Eq. 11) boundary conditions are respectively given by:

$$w=0, \qquad M_x=0 \quad \text{at } x=0,\,L, \tag{10}$$

$$N_x=0, \qquad v=0 \quad \text{at } x=0,\,L. \tag{11}$$

For a formulation based on a stress function, the in-plane boundary conditions are satisfied on the average by introducing the following conditions, as justified, for example, in (Amabili, 2008; Amabili et al, 1999; Stavridis, 1988; Breslavsky and Avramov, 2013; Del Prado et al, 2014)

$$\int_0^{2\pi} N_x R\,d\theta=0\,, \text{ at } x=0,\,L, \tag{12}$$

$$\int_0^{2\pi}\int_0^{L} N_{x\theta} R\,d\theta=0\,, \text{ at } x=0,\,L. \tag{13}$$

Equation (12) assures a zero axial force N_x on the average, while Eq. (13) is satisfied when u and w are continuous in θ on average, and v=0 on average at both ends (Amabili et al, 1999).

To determine the perturbation pressure on the shell wall, the Païdoussis and Denise (Paidoussis, 2004) model will be adopted. In this model, linear potential theory is used to describe the effect of the internal axially flowing fluid. The fluid is assumed to be incompressible and non-viscous and the flow to be isentropic and irrotational. The irrotationality property is the condition for the existence of a scalar potential function Ψ, from which the velocity may be written as

$$V=-\nabla\Psi\,. \tag{19}$$

This potential function is equal to $\Psi=-U\,x+\Phi$, where the first term is associated with the undisturbed mean flow velocity U, and the second term, the unsteady component Φ, is associated with shell motion. The function Φ must satisfy the Laplace equation and the impenetrability condition at the shell-fluid interface.

The potential function satisfies the continuity equation. Following the procedure presented in previous studies (Amabili et al, 2000; Paidoussis, 2004), the perturbation pressure on the shell wall is found to be

$$P_h = \rho_F \frac{L}{m\pi} \frac{\mathrm{I}_n(m\pi R/L)}{\mathrm{I}_n^{'}(m\pi R/L)} \left(\frac{\partial^2 w}{\partial t^2} \right), \tag{21}$$

Where ρ_F is the fluid density I_n is the nth order modified Bessel function and $\mathrm{I}_n^{'}$ is its derivative with respect to its argument.

In this work, two modal expansions for the lateral displacements $w(x,\theta,t)$, satisfing the out-of-plane boundary conditions (10) in terms of the circumferential and axial variables were adopted (Amabili et al, 1999), one for the empty cylindrical shells and other for the fluid-filled shell.

The modal expansion for the empty shell containing six degrees of freedom, containing the basic vibration mode, the companion mode and four axi-symmetric modes is given by:

$$\begin{aligned} w(x,\theta,t) = {} & \xi_1(t) h \sin\left(\frac{m\pi x}{L}\right)\cos(n\theta) + \xi_2(t) h \sin\left(\frac{m\pi x}{L}\right)\sin(n\theta) + \\ & \xi_3(t) h \sin\left(\frac{m\pi x}{L}\right) + \xi_4(t) h \sin\left(\frac{3m\pi x}{L}\right) + \xi_5(t) h \sin\left(\frac{5m\pi x}{L}\right) + \\ & \xi_6(t) h \sin\left(\frac{7m\pi x}{L}\right) \end{aligned} \tag{14}$$

Where $\xi_1(t)$, $\xi_2(t)$, $\xi_3(t)$, $\xi_4(t)$, $\xi_5(t)$ and $\xi_6(t)$ are the time-dependent non-dimensional modal amplitudes, where the shell thickness h has been used as non-dimensionalization parameter.

The modal expansion for the empty shell containing eight degrees of freedom, containing the basic vibration mode, the companion mode, two gyroscopic modes and four axi-symmetric modes is given by:

$$\begin{aligned} w(x,\theta,t) = {} & \xi_1(t) h \sin\left(\frac{m\pi x}{L}\right)\cos(n\theta) + \xi_2(t) h \sin\left(\frac{m\pi x}{L}\right)\sin(n\theta) + \\ & \xi_3(t) h \sin\left(2\frac{m\pi x}{L}\right)\cos(n\theta) + \xi_4(t) h \sin\left(2\frac{m\pi x}{L}\right)\sin(n\theta) + \\ & \xi_5(t) h \sin\left(\frac{m\pi x}{L}\right) + \xi_6(t) h \sin\left(\frac{3m\pi x}{L}\right) + \xi_7(t) h \sin\left(\frac{5m\pi x}{L}\right) + \\ & \xi_8(t) h \sin\left(\frac{7m\pi x}{L}\right) \end{aligned} \tag{15}$$

where $\xi_1(t)$, $\xi_2(t)$, $\xi_3(t)$, $\xi_4(t)$, $\xi_5(t)$, $\xi_6(t)$, $\xi_7(t)$ and $\xi_8(t)$ are the time-dependent non-dimensional modal amplitudes, where the shell thickness h has been used as non-dimensionalization parameter.

The solution for the stress function may be written as $F = F_h + F_p$, where F_h is the homogeneous solution and F_p, the particular solution. The particular solution F_p is obtained analytically by substituting the assumed form of the lateral displacement, Eq. (14) or Eq. (15), on the right-hand side of the compatibility equation, Eq. (9), and by solving the resulting partial differential equation together with the relevant boundary and continuity conditions.

The homogeneous part of the stress function can be written as [22]:

$$F_h = \frac{1}{2}\tilde{N}_x R^2 \theta^2 + \frac{1}{2}x^2\left\{\tilde{N}_\theta - \frac{1}{2\pi R L}\int_0^L\int_0^{2\pi}\frac{\partial^2 F_p}{\partial x^2} R\, d\theta\, dx\right\} - \tilde{N}_{x\theta} xR\theta \tag{16}$$

where $\tilde{N}_x$, $\tilde{N}_\theta$ and $\tilde{N}_{x\theta}$ are the in-plane restrain stresses at the ends of the shell.

Upon substituting the modal expressions for F and $w(x, \theta, t)$ into the equation of motion, Eq. (8), and applying the Galerkin method, a set of six non-linear ordinary differential equations is obtained in terms of the time-dependent modal amplitudes, $\xi_i(t)$.

In analysis, the following non-dimensional parameters are used for time and shell frequency:

$$\tau = \omega_o t\,, \tag{16}$$

$$\Omega_L = \omega_L / \omega_o\,. \tag{17}$$

3 NUMERICAL RESULTS

Consider a simply supported viscoelastic cylindrical shell with the following physical and geometrical properties: R = 0.2 m, L = 0.4 m, h = 0.002 m, ρ = 1340.0 kg/m^3, ρ_F = 1000.0 kg/m^3, ν = 0.195, E = 45.5e9 N/m^2 [26], ζ = 0.001. Thus one has the geometrical ratios: L/R = 2.0 and R/h = 100.0. For this shell the lowest natural frequencies are ω_o = 3165.03 rad/sec (empty shell) and ω_o = 897.59 rad/sec (fluid-filled shell) which are associated to a mode shape with m = 1 longitudinal half-wave and n = 5 circumferential waves.

To try to understand the influence of both the viscoelastic dissipation parameter and the lateral load on the non-linear dynamic behavior of the shell, several resonance curves, for empty and fluid-filled shell, have been computed. The bifurcation diagrams were obtained using both force brute and continuation techniques and considering the excitation frequency as control parameter. The nondimensional coefficient of the amplitude of the lateral load F_L was varied with the following values: 0.2 and 0.5. For the coefficient of the viscoelastic dissipation parameter of the Kelvin-Voigt model η, the following values were assumed: 0.0, 1.0e-5, 2.0e-5, 3.0e-5 and 1.0e-4 s. In diagrams black curves represent stable oscillations and gray curves represent unstable oscillations.

Figure 2 displays the resonance curves of driven mode for an empty shell considering an excitation level of F_L = 0.2. As it can be observed in Fig. 2(a), for a shell without viscoelasticity (η = 0.0), as the frequency parameter Ω_L is increased the shell displays small amplitude period one oscillations (1T). At an excitation frequency near Ω_L = 0.90 the shell displays a jump from small to very large amplitude oscillations displaying softening behavior. Here it must be observed that the vibration amplitude is so large as to be outside the accuracy limit of the Donnell shallow-shell theory. As the value of Ω_L is increased, the shell shows a reduction of the vibration amplitude.

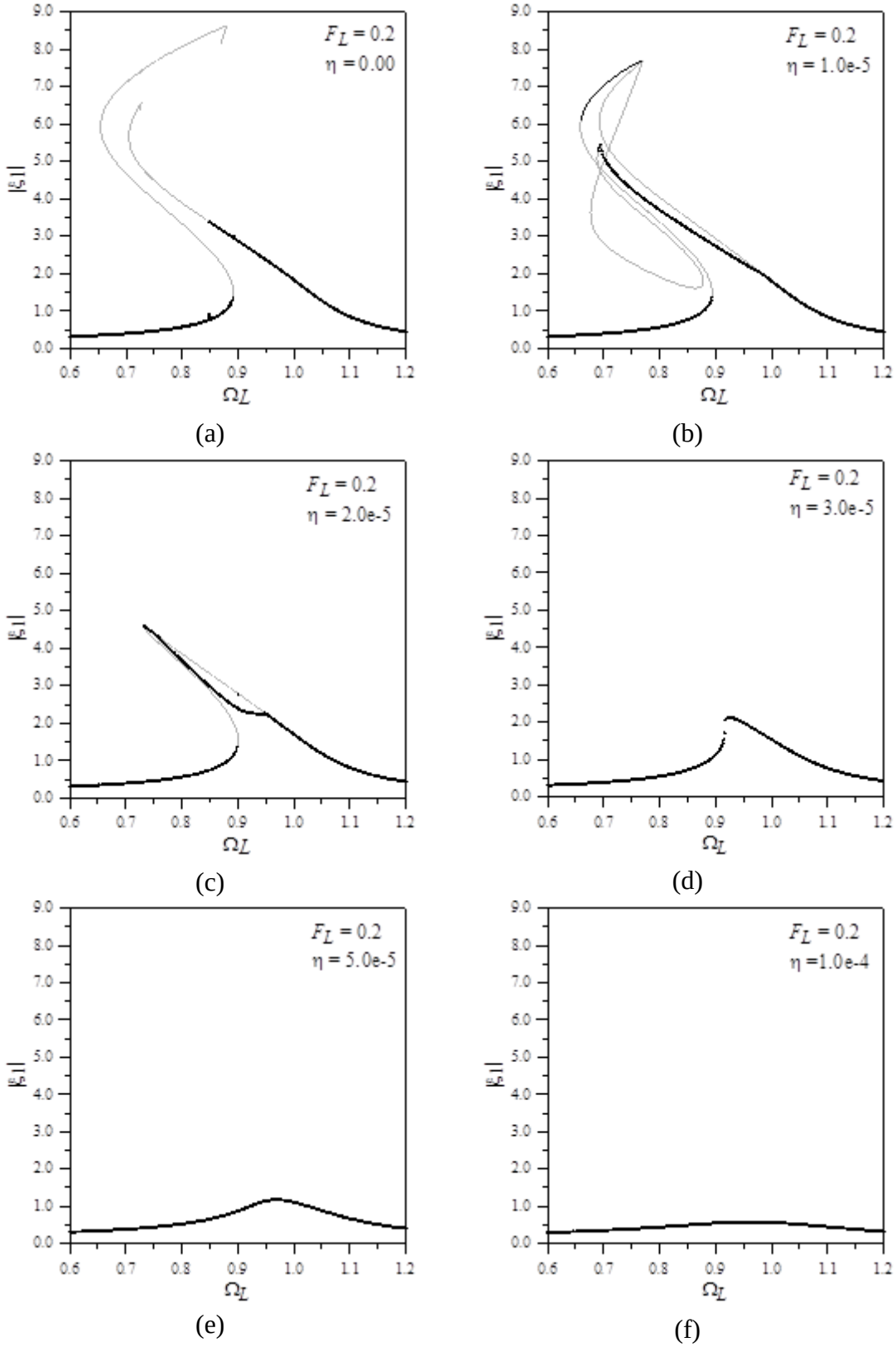
$F_L = 0.2$
$\eta = 0.00$
$F_L = 0.2$
$\eta = 1.0e\text{-}5$
$F_L = 0.2$
$\eta = 2.0e\text{-}5$
$F_L = 0.2$
$\eta = 3.0e\text{-}5$
$F_L = 0.2$
$\eta = 5.0e\text{-}5$
$F_L = 0.2$
$\eta = 1.0e\text{-}4$
$|\xi_1|$
Ω_L
(a)
(b)
(c)
(d)
(e)
(f)

Figure 2 – Resonance curves of the empty shell for drive mode considering F_L = 0.2. (a) η = 0.0 s; (b) η = 1.0e-5 s; (c) η = 2.0e-5 s; (d) η = 3.0e-5 s; (e) η = 5.0e-5 s; (e) η = 1.0e-4 s.

Now, when the viscoelastic dissipation parameter is considered ($\eta \neq 0$), the non-linear behavior of the shell is strongly influenced. Figure 2(b) shows the resonance curve for η = 1.0e-5 s and as the frequency parameter Ω_L is increased, the shell displays small amplitude 1T period oscillations. Again at a value close to Ω_L = 0.90, the shell displays a jump to large amplitude oscillations with strong softening behavior. It is also possible to observe that the softening region of the response has complicated non-linear unstable paths while a stable path displaying hardening behavior is observed for large amplitude oscillations. Then, for Ω_L between 0.72 and 0.77, the shell displays three different stable equilibrium points, which means that there will be three stable attractors. At large amplitude a folding of the backbone curve (turning point) associated with large bending effects occurs.

When η is increased to 2.0e-5 s as shown if Fig. 2(c), the resonance curve is again affected and it shows softening behavior but with smaller vibration amplitudes than for the previous case. Also, in Figs. 2(b) and 2(c) for Ω_L=1.0 the shell displays a bifurcation point where the unstable path is linked to the large vibrations amplitudes path.

When η is increased to 3.0e-5 s, 5.0e-5 s or to 1.0e-4 s, as the frequency parameter is increased, the shell displays only small amplitude vibrations with no softening behavior, as observed in Fig. 2(d), Fig. 2(e) and 2(f).

Now, when the steady internal fluid is considered, Fig. 3 displays the resonance curves of the driven mode considering an excitation level of F_L = 0.2 and increasing values of the excitation frequency.

Figure 3(a) depicts the resonance curve for η = 0.0 s and as can be observed, as the frequency parameter Ω_L is increased the shell displays small amplitude period one oscillations (1T). At an excitation frequency near Ω_L = 0.90 the shell shows a jump from small to large amplitude oscillations displaying a kind of softening behavior, if Fig. 3(a) is compared with Fig. 2(a) it is possible to observe the strong influence of internal fluid where the global dynamic behavior is completely changed. The fluid reduced the jump of the shell as well as the altered the softening behavior.

Now, Fig. 3(b) and Fig. 3(c) display the resonance curve for η = 1.0e-5 s and η = 2.0e-5 s and as can be observed, there is a small jump near Ω_L = 0.90 with no softening behavior in both cases. When the viscoelastic dissipation parameter is increased, Fig. (d), Fig. (e) and Fig. (f) depict only small amplitude oscillations with no softening behavior. If the resonance curves of empty and fluid-filled shell are compared, now it is clear the effect of internal fluid where the fluid-filled shell shows smaller amplitudes than the empty shell with only small jumps for lower values of viscoelastic dissipation parameter.

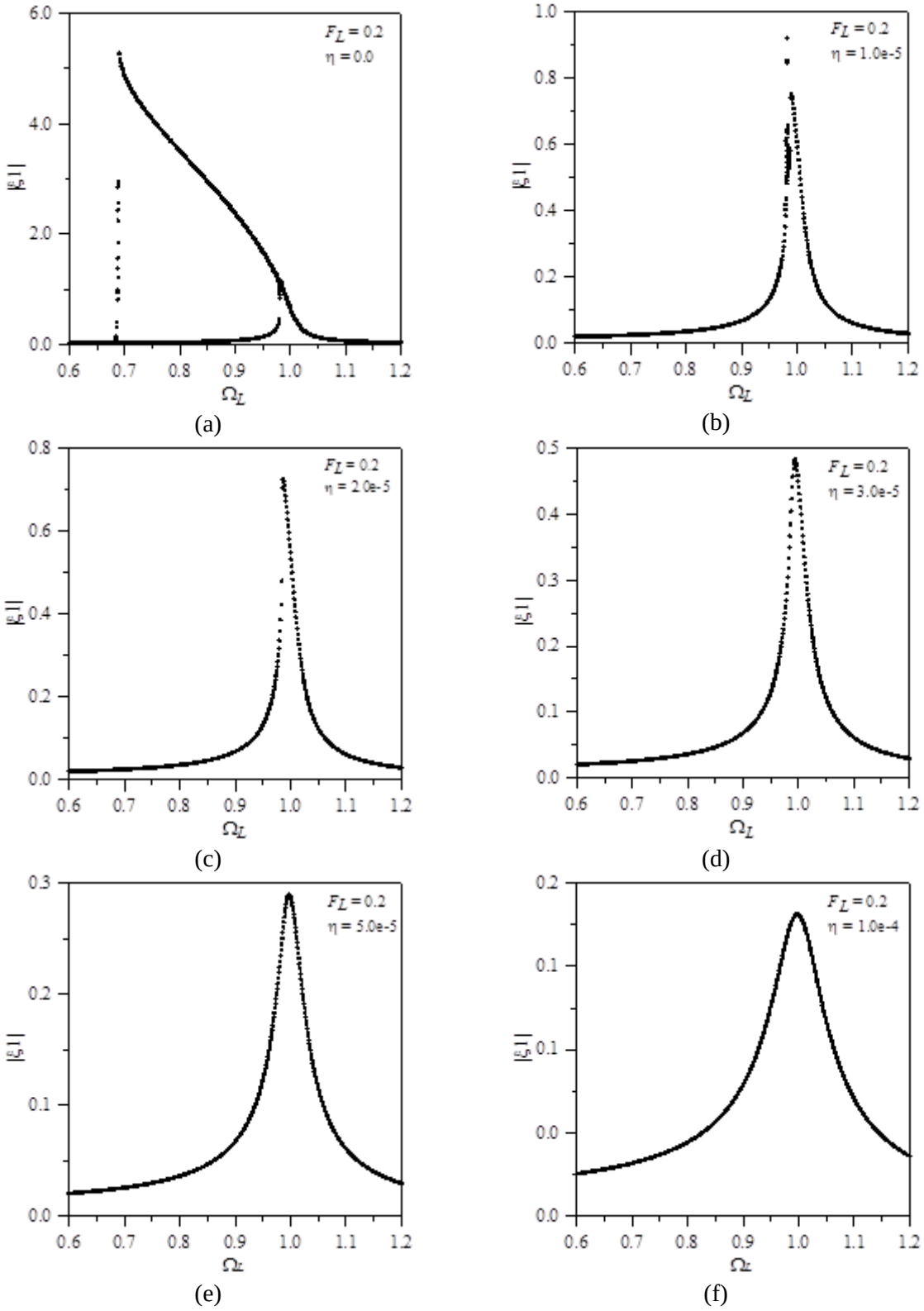

Figure 3 – Resonance curves of the fluid-filled shell for drive mode considering F_L = 0.2. (a) η = 0.0 s; (b) η = 1.0e-5 s; (c) η = 2.0e-5 s; (d) η = 3.0e-5 s; (e) η = 5.0e-5 s; (e) η = 1.0e-4 s.

Figure 4 displays the resonance curves of the empty shell for $F_L = 0.5$.. As it can be observed in Fig. 4(a) with $\eta = 0.0$, for initial increasing values of Ω_L the shell displays growing small amplitude oscillations and, at approximately $\Omega_L = 0.78$ the shell starts to display a window of large amplitude chaotic oscillations until $\Omega_L = 0.87$. After this point the shell shows decreasing oscillating amplitudes as the frequency parameter is increased. If η goes up to 1.0e-5 s as observed in Fig 4(b), again the behavior of the shell if strongly affected. The shell displays softening behavior with large amplitude oscillations and three stable attractors (small, medium and large amplitude oscillations) for Ω_L between 0.73 and 0.80. Fig 4(c) shows the resonance curve for $\eta = 2.0$e-5 s; in this case the non-linear behavior of the shell is altered and the shell displays complicated softening unstable paths but with smaller amplitudes than for $\eta = 1.0$e-5 s. If $\eta = 3.0$e-5 s, as shown in Fig. 4(d), the shell depicts softening behavior with a stable path of large amplitude oscillations for Ω_L varying from 0.63 to 0.75. Also, it is possible to observe the coexistence of a window of quasi-periodic oscillations for Ω_L varying between 0.71 and 0.77. Figure 4(e) depicts the resonance curve for $\eta = 5.0$e-5 s displaying simple softening behavior with stable and unstable paths but, with smaller vibration amplitudes than in previous cases. Finally, Fig. 4(e) displays the resonance curve for $\eta = 1.0$e-4 s. In this case, the shell displays only small amplitude oscillations with no unstable paths.

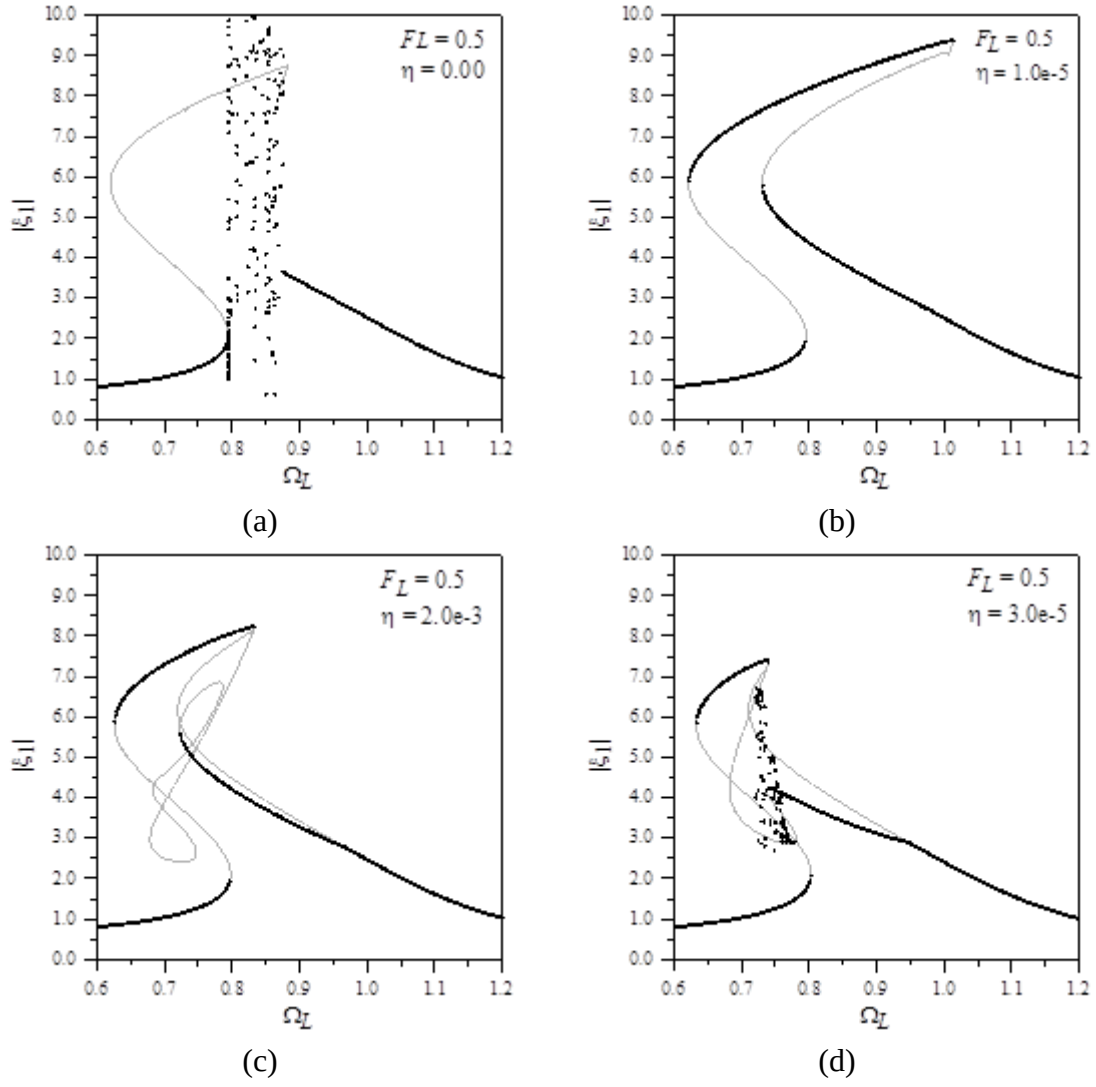

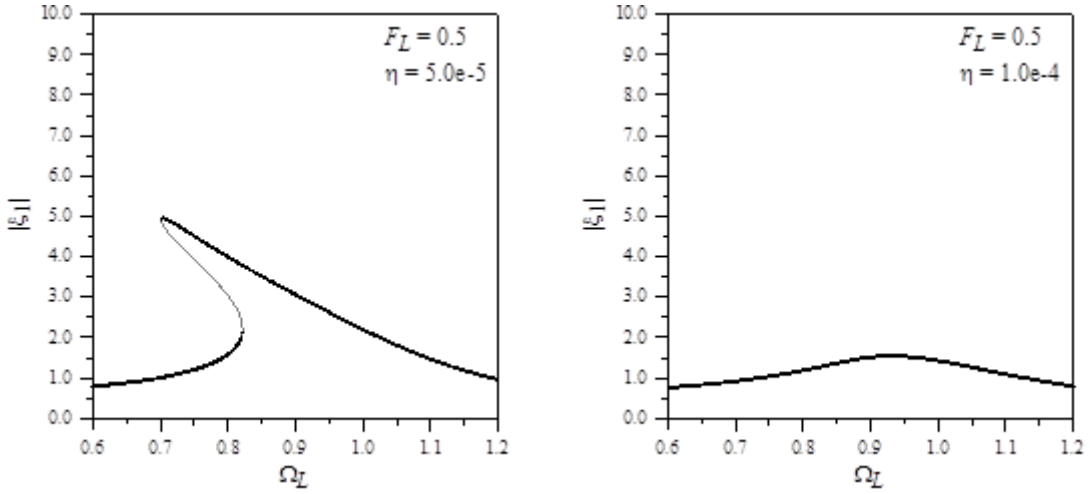

Figure 4 - Resonance curves of empty shell for driven mode considering F_L = 0.5. (a) η = 0.0 s; (b) η = 1.0e-5 s; (c) η = 2.0e-5 s; (d) η = 3.0e-5 s; (e) η = 5.0e-5 s; (f) η = 1.0e-4 s.

Finally, Fig. 5 displays the resonance curves of the fluid-filled shell for $F_L = 0.5$ versus the frequency parameter Ω_L. As it can be observed in Fig. 5(a) with $\eta = 0.0$, for initial increasing values of Ω_L the shell displays growing small amplitude oscillations and, at approximately $\Omega_L = 0.80$ the shell displays a jump to large amplitude oscillations with softening behavior. If η goes up to 1.0e-5 s as observed in Fig 5(b), again the behavior of the shell if strongly affected. The shell displays softening behavior with medium amplitude oscillations and the coexistence of two stable attractors (small and medium).

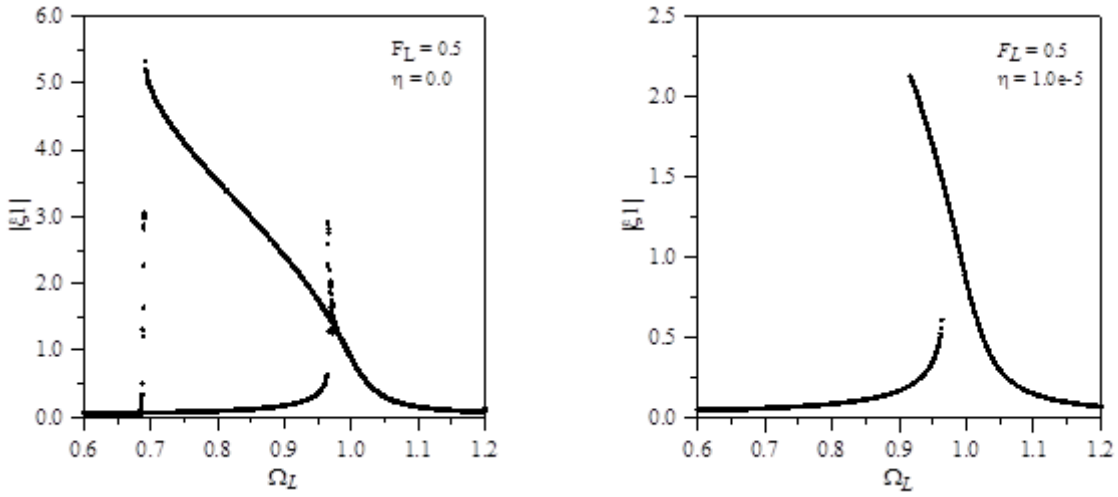

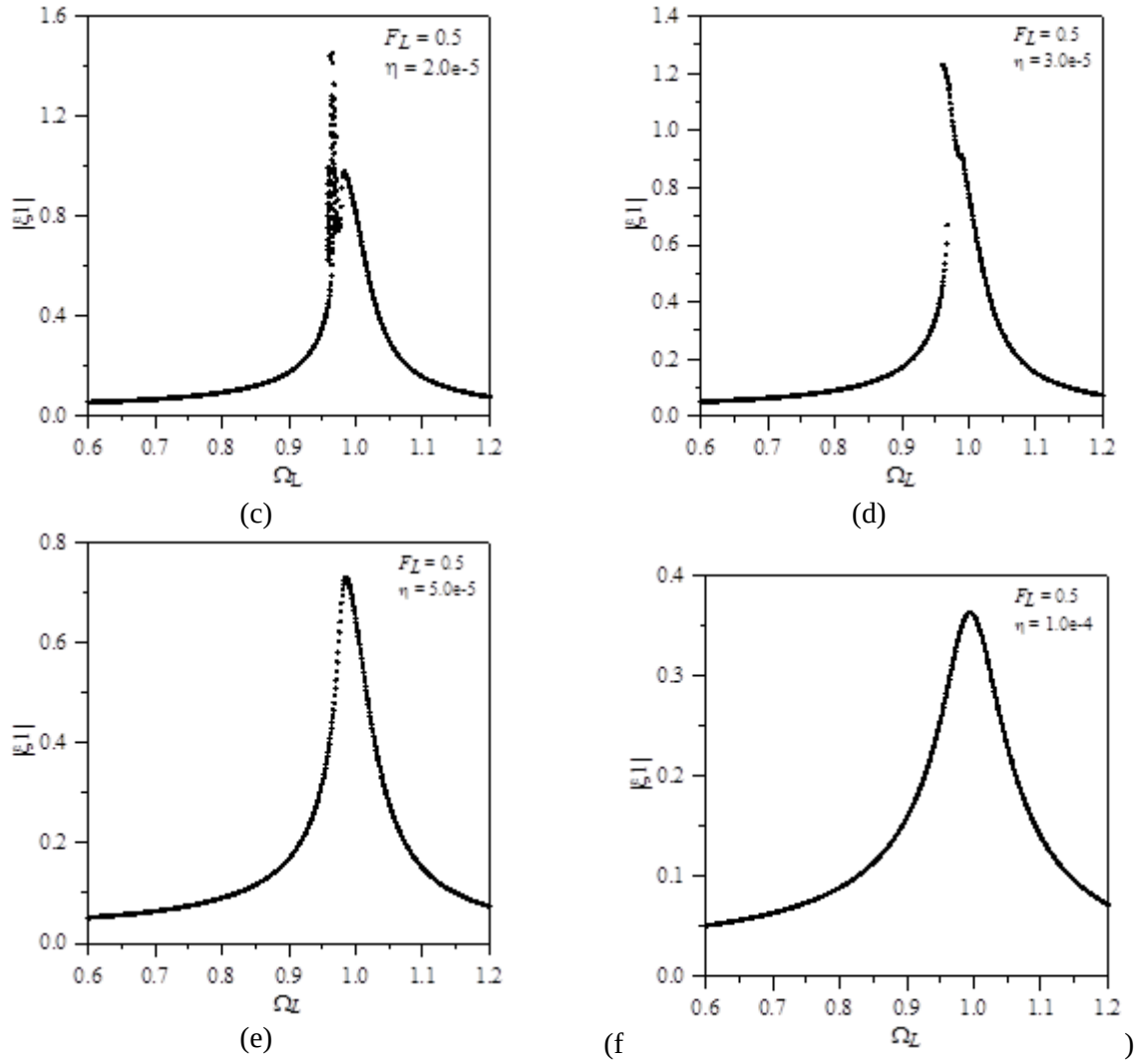

Figure 5 – Resonance curves of fluid-filled shell for driven mode considering F_L = 0.5. (a) η = 0.0 s; (b) η = 1.0e-5 s; (c) η = 2.0e-5 s; (d) η = 3.0e-5 s; (e) η = 5.0e-5 s; (f) η = 1.0e-4 s.

Now, Fig 5(c) shows the resonance curve for η = 2.0e-5 s; in this case the non-linear behavior of the shell is altered and the shell displays complicated softening unstable paths but with smaller amplitudes than for η = 1.0e-5 s. If η = 3.0e-5 s, as shown in Fig. 4(d), the shell depicts softening behavior with a stable path of large amplitude oscillations for Ω_L varying from 0.63 to 0.75. Also, it is possible to observe the coexistence of a window of quasi-periodic oscillations for Ω_L varying between 0.71 and 0.77. Figure 4(e) depicts the resonance curve for η = 5.0e-5 s displaying simple softening behavior with stable and unstable paths but, with smaller vibration amplitudes than in previous cases. Finally, Fig. 4(e) and Fig. 4(f) display the resonance curve for η = 5.0e-5 s and η = 1.0e-4 s. In these cases, as can be observed, the shell displays only small amplitude oscillations with no unstable paths.

As can be observed, when comparing Fig. 4 and Fig. 5, there is a great influence of both viscosity parameter and internal fluid on the global non-linear dynamic of the shell. If an empty shell is considered, it is possible to observe stable, unstable and chaotic oscillations and, when a fluid-filled shell is considered, it is possible to observe stable paths and only a small window of chaotic oscillations. When the viscosity parameter is increased, only stable small amplitude vibrations can be observed for the fluid-filled shell.

4 CONCLUDING REMARKS

In this work, the non-linear vibrations analysis of a viscoelastic Kelvin-Voigt simply supported cylindrical empty and fluid- filled shell, subjected to lateral time dependent loads is analyzed. To model the shell, the Donnell's non-linear shallow shell theory is applied and an expansion with 6 and 8 degrees of freedom is used to describe the lateral displacements. Results show that the inclusion of the viscoelastic dissipation parameter η of the Kelvin-Voigt material and internal fluid affect strongly the non-linear response of the shell.

It is possible to see that the viscoelastic dissipation parameter and fluid influence the number of attractors of the non-linear response giving rise to the co-existence of stable, quasi-periodic and chaotic oscillations. When fluid is considered, the non-linear dynamic response is altered and the shell starts to display smaller vibration amplitudes than the empty shell.

For higher values of the dissipation parameter, the shell only displays small amplitude vibrations without jumps, hysteresis and multiple solutions. This illustrates the beneficial effect of viscoelasticity in reducing large amplitude unwanted vibrations.

ACKNOWLEDGEMENTS

This work was made possible by the support of the Brazilian Ministry of Education – CNPq and FAPERJ-CNE and NSERC Discovery Grant, Discovery Accelerator Supplement and Canada Research Chair.

REFERENCES

Alijani F, Amabili M., 2013. Non-linear vibrations of shells: A literature review from 2003 to 2013. *International Journal of Non-Linear Mechanics*, pp. 58:233–257.

Amabili M., 2008. *Nonlinear Vibrations and Stability of Shells and Plates*. 1st ed. New York: Cambridge University Press.

Amabili M., Pellicano F, Païdoussis M.P., 1999. Non-linear dynamics and stability of circular cylindrical shells containing flowing fluid. Part I: Stability. Journal of Sound and Vibration. vol. 225, pp.655-699.

Amabili, M. Pellicano, F. and Païdoussis, M.P., 2000. Non-linear dynamics and stability of circular cylindrical shells containing flowing fluid. Part III: truncation effect without flow and experiments, *Journal of Sound and Vibration* 237. pp. 617–640.

Antman SS, Lacarbonara W., 2009. Forced Radial Motions of Nonlinearly Viscoelastic Shells. *Journal of Elasticity*, vol. 96, pp. 155–190.

Breslavsky I.D, Avramov K.V., 2013. Effect of boundary condition nonlinearities on free large-amplitude vibrations of rectangular plates. *Nonlinear Dynamics*, vol. 74, pp.615-627.

Cheng C, Zhang N., 2001. Dynamic behavior of viscoelastic cylindrical shells under axial pressure, *Applied Mathematics and Mechanics*, vol. 2, pp. 1-9.

Cederbaum G, Touati D., 2002, Postbuckling analysis of imperfect non-linear viscoelastic cylindrical panels. *International Journal of Non-Linear Mechanics*, vol. 37, pp.757–762.

Del Prado Z, Argenta A.L, Da Silva F, Gonçalves P.B., 2014, The effect of material and geometry on the non-linear vibrations of orthotropic circular cylindrical shells. *International Journal of Non-Linear Mechanics*, vol. 66, pp. 75–86.

Eshmatov B.K, Khodjaev D.A., 2007a, Non-linear vibration and dynamic stability of a viscoelastic cylindrical panel with concentrated mass. *Acta Mechanica*, vol. 190, pp.165–183.

Eshmatov B.K., 2007b, Nonlinear vibrations of viscoelastic cylindrical shells taking into account shear deformation and rotatory inertia. *Nonlinear Dynamics*, vol. 50, pp. 353–361.

Eshmatov B.K., 2007c, Dynamic stability of viscoelastic circular cylindrical shells taking into account shear deformation and rotatory inertia. *Applied Mathematics and Mechanics, vol.* 28, pp. 1319–1330.

Eshmatov B.K, Khodzhaev D.A., 2007d, Non-linear vibration and dynamic stability of a viscoelastic cylindrical panel with concentrated mass. *Acta Mechanica*, vol. 190, pp. 165–183.

Eshmatov B.K, Khodzhaev D.A., 2008, Dynamic stability of a viscoelastic cylindrical panel with concentrated masses. *Strength of Materials*, vol. 40, pp. 491–502.

Eshmatov B.K., 2009, Nonlinear vibrations and dynamic stability of a viscoelastic circular cylindrical shell with shear strain and inertia of rotation taken into account. *Mechanics of Solids*, vol. 44, pp. 421–434.

Esmailzade E, Jalali M.A., 1999, Nonlinear Oscillations of Viscoelastic Rectangular Plates. *Nonlinear Dynamics*, vol. 18, pp. 311–319.

Lacarbonara W, Antman S.S., 2012, Parametric instabilities of the radial motions of non-linearly viscoelastic shells under pulsating pressures. *International Journal of Non-Linear Mechanics*, vol. 47, pp. 461–472.

Mohammadi F, Sedaghati R., 2012, Vibration analysis and design optimization of viscoelastic sandwich cylindrical shell. *Journal of Sound and Vibration*, vol. 331, pp. 2729–2752

Païdoussis, M.P., 2004, *Fluid Structure Interactions. Slender Structures and Axial Flow, Vol. 2*, Elsevier Academic Press, London.

Shina W., Leeb S, Ohc I, Lee I., 2009, Thermal post-buckled behaviors of cylindrical composite shells with viscoelastic damping treatments. *Journal of Sound and Vibration*, vol. 323, pp. 93–111.

Stavridis L, Armenàkas A., 1988, Analysis of Shallow Shells with Rectangular Projection: Theory. *ASCE Journal of Engineering Mechanics*, vol. 114, pp. 923–942.